A&A 534, A64 (2011)
DOI: 10.1051/0004-6361/201117494

Astronomy & Astrophysics

Hydrogenation of solid hydrogen cyanide HCN and methanimine CH_2NH at low temperature

P. Theule[1], F. Borget[1], F. Mispelaer[1], G. Danger[1], F. Duvernay[1], J. C. Guillemin[2], and T. Chiavassa[1]

[1] Université de Provence, Laboratoire de Physique des Interactions Ioniques et Moléculaires, Centre de St-Jérôme, Avenue Escadrille Normandie-Niémen, 13397 Marseille, France
e-mail: patrice.theule@univ-provence.fr
[2] Sciences Chimiques de Rennes, École Nationale Supérieure de Chimie de Rennes, CNRS, UMR 6226, Avenue du Général Leclerc, CS 50837, 35708 Rennes Cedex 7, France

Received 16 June 2011 / Accepted 7 August 2011

ABSTRACT

Context. Hydrogenation reactions dominate grain surface chemistry in dense molecular clouds and lead to the formation of complex saturated molecules in the interstellar medium.
Aims. We investigate in the laboratory the hydrogenation reaction network of hydrogen cyanide HCN.
Methods. Pure hydrogen cyanide HCN and methanimine CH_2NH ices are bombarded at room temperature by H-atoms in an ultra-high vacuum experiment. Warm H-atoms are generated in an H_2 plasma source. The ices are monitored with Fourier-transform infrared spectroscopy in reflection absorption mode. The hydrogenation products are detected in the gas phase by mass spectroscopy during temperature-programmed desorption experiments.
Results. HCN hydrogenation leads to the formation of methylamine CH_3NH_2, and CH_2NH hydrogenation leads to the formation of methylamine CH_3NH_2, suggesting that CH_2NH can be a hydrogenation-intermediate species between HCN and CH_3NH_2.
Conclusions. In cold environments the HCN hydrogenation reaction can produce CH_3NH_2, which is known to be a glycine precursor, and to destroy solid-state HCN, preventing its observation in molecular clouds ices.

Key words. astrochemistry – ISM: molecules – molecular processes

1. Introduction

Surface hydrogenation reactions play an important role in the evolution of molecules on interstellar ices, especially at low temperatures in dense molecular clouds where the secondary photon field is very weak and where hydrogen atoms have an important residence time on the surface. Very few studies have been carried out on these hydrogenation reactions. Hiraoka et al. (1994), Watanabe et al. (2002), and Fuchs et al. (2009) show how H_2CO and CH_3OH can be formed from the hydrogenation of CO. The solid-state H_2O formation routes from the hydrogenation of the oxygen atom (Hiraoka et al. 1998; Dulieu et al. 2010), from the dioxygen molecule (Miyauchi et al. 2008; Ioppolo et al. 2008; Matar et al. 2008) and from the ozone molecule (Mokrane et al. 2009; Romanzin et al. 2011) have been extensively studied. The formation of C_2H_5OH, CH_3OH, H_2CO and CH_4 from the hydrogenation of CH_3CHO has also been studied by (Bisschop et al. 2007), as well as the formation of HCOOH from the hydrogenation of a $CO{:}O_2$ mixture (Ioppolo et al. 2011). It is important to have a detailed reaction network of these hydrogenation processes because they have reaction rates faster than thermal or photochemical reactions at low temperatures and under a weak radiation field. In addition, the residence time of the hydrogen atoms on ice surface makes these reactions dominant in grain surface chemistry at low temperature. Moreover, HCN is a key molecule in interstellar chemistry because it is the simplest molecule containing a CN moiety, which is a prerequisite to form amino-acids (Ferris et al. 1984).

We bombarded solid hydrogen cyanide HCN and methanimine CH_2NH with warm H-atoms generated from an H_2 plasma source to obtain the hydrogenation reaction network of HCN at low temperature. We used Fourier-transform reflection absorption infrared spectroscopy (RAIRS) to monitor the ice analog composition, and mass spectrometry to detect the hydrogenation products during temperature-programmed desorption experiments. We show that HCN can be hydrogenated into fully saturated methylamine CH_3NH_2, and that methanimine CH_2NH can also be hydrogenated into CH_3NH_2. It has been shown that methylamine CH_3NH_2 can thermally react with CO_2 in the solid phase to form a carbamate, which can be converted in a glycine salt under VUV irradiation. This glycine salt eventually thermally desorbs as gas-phase-neutral glycine NH_2CH_2COOH (Bossa et al. 2009).

2. Experimental

The experiments were performed using our RING experimental set-up as described elsewhere (Theule et al. 2011). A polished copper surface is maintained at 15 K using a closed-cycle helium cryostat (ARS Cryo, model DE-204 SB, 4 K cryogenerator) within a high-vacuum chamber at a few 10^{-9} mbar. Ice analogs are formed by spraying a room-temperature gas onto the polished copper surface. The infrared spectra are recorded by means of Fourier-transform reflection absorption infrared Spectroscopy (FT-RAIRS) using a Vertex 70 spectrometer with a MCT detector. A typical spectrum has a 1 cm^{-1} resolution and is averaged

over a few hundred interferograms. Final hydrogenation products are detected in the gas phase after thermal desorption from the substrate, which is warmed using a heating resistance. The sample temperature is measured with a DTGS 670 Silicon diode with a 0.1 K uncertainty, and controlled using a Lakeshore Model 336 temperature controller. Gas-phase species are detected by means of mass spectrometry, using a Hiden HAL VII RGA quadrupole mass spectrometer. The ionization source is a 70 eV impact electronic source and the mass spectra are recorded between 1 and 60 amu. In a typical temperature-programmed desorption experiment (TPD), the mass spectra are recorded as the products are being desorbed during a 5 K/min temperature ramp.

Warm atomic hydrogen is produced from a molecular hydrogen plasma source. The plasma is generated from a 2.45 GHz microwave discharge (Opthos Instruments Inc.) within an Evenson cavity (Fehsenfeld et al. 1965) where molecular hydrogen gas is flowing in a 13 mm diameter pyrex tube at approximately 5×10^{-2} mbar. A few microns diameter 5 mm long pyrex capillary allows one to extract hydrogen atoms from the plasma. Charged particles (H^+, H_2^+, e^-,...) recombine quickly within the capillary because of its small diameter. However, we do not know the cation-electron recombination rate within the capillary and thus the overall hydrogen atom yield at the capillary output. At the output of the capillary, a 13 mm diameter pyrex elbow tube prevents photons generated in the plasma from reaching the ice-analog sample. Because the mean free path of the hydrogen atoms is much smaller than the dimensions of the elbow tube, hydrogen atoms undergo several collisions in the room-temperature tube, which means that the kinetic energy of the warm hydrogen atoms impinging on the ice analog sample must be around 300 K. We calibrated the atomic hydrogen flux by hydrogenating CO following Watanabe et al. (2002). A CO ice at 15 K is exposed to the hydrogen beam and the H_2CO band at 1720 cm^{-1} is monitored along with time using FTIR spectroscopy. In our experimental conditions, the formed quantity of H_2CO reaches the plateau after approximately 150−200 min of exposure. Following Watanabe et al. (2002), we can make a rough estimate of our H flux to few 10^{14} cm^{-2} s^{-1}. The tube is directly connected to the high-vacuum chamber, facing the sample holder, so that the pressure within the chamber is a few 10^{-6} mbar when a 5×10^{-2} mbar molecular hydrogen pressure is at the input of the capillary tube. A 15 K temperature is chosen during the hydrogenation experiments to prevent condensation of H_2 on the surface. We chose a sufficiently low temperature to allow the hydrogen atoms to remain long on the surface but the temperature was initially high enough to allow hydrogen atoms to have a high mobility to move on the surface and penetrate as deep as possible into the bulk of the ice, and also to overcome a possible activation barrier at hydrogenation, if a Langmuir-Hinshelwood mechanism were present. A typical hydrogenation experiment lasts around three hours, which corresponds to a dose of 10^{18} cm^{-2} of warm H-atoms.

The HCN monomer is synthesized from the thermal reaction of potassium cyanide KCN and an excess of stearic acid $CH_3(CH_2)_{16}COOH$ in a primary pumped vacuum line, as described in Gerakiness et al. (2004). The methanimine CH_2NH monomer was obtained from the dehydrocyanation of aminoacetonitrile following the synthesis protocol decribed in Guillemin and Denis (1988). Briefly, in a first step, aminoacetonitrile NH_2CH_2CN is synthesized from aminoacetonitrile hydrogensulfate $NCCH_2NH_3^+HSO_4^-$ in powder suspended in dichloromethane CH_2Cl_2, by bubbling ammonia in the solution to neutralize the acid. Then, aminoacetonitrile is thermolyzed at 600 °C to form methanimine and hydrogen cyanide. The latter is selectively trapped on KOH and the methanimine monomer is trapped in liquid nitrogen. Methanimine is a kinetically unstable compound that can be kept few hours in dry ice but indefinitely in liquid nitrogen.

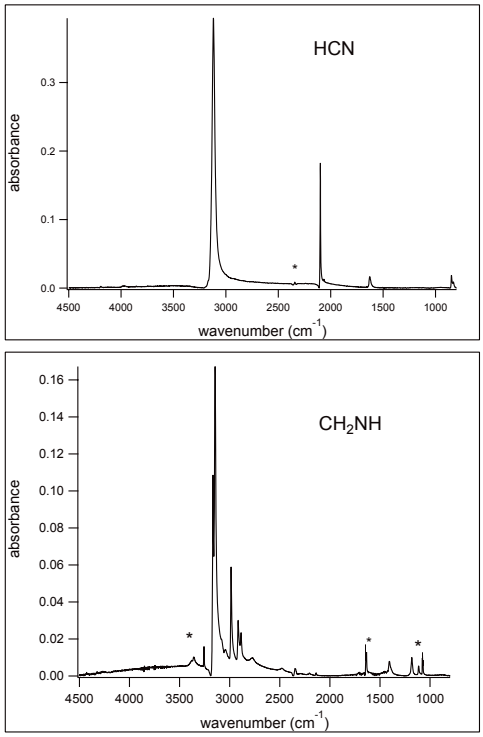

Fig. 1. Pure hydrogen cyanide HCN (*top*) and methanimine CH_2NH (*bottom*) infrared spectrum at $T = 15$ K before hydrogenation. Synthesis by-products are observed from their bands marked with an asterisk. The bands at 1010, 1628, and 3377 cm^{-1} correspond to NH_3 remaining from the CH_2NH synthesis, and the band at 2349 cm^{-1} corresponds to CO_2 issued from the decomposition of stearic acid during the HCN synthesis.

3. Results

3.1. Hydrogenation of pure hydrogen cyanide HCN

Gas-phase HCN is sprayed onto the polished copper surface maintained at 15 K. After deposition, the purity of the sample is checked on an IR spectrum, as seen in Fig. 1. Very little CO_2 impurity originating from the HCN synthesis is present in the spectra. The IR bands of the different species are listed in Table 1 along with their corresponding assignments.

Solid HCN is exposed to the warm atomic hydrogen beam at 15 K during a fixed amount of time. Three hydrogenation experiments are performed during 20 min, one hour, and three hours, respectively. The three-hours experiment was repeated several times to check for the reproducibility. A reference experiment was performed where H_2 was kept a long time at 15 K without being exposed to the hydrogen beam. We do not observe hydrogenation products in the IR spectra after hydrogenation, owing to a low hydrogenation yield. To detect the hydrogenation products the sample is warmed to room-temperature during a TPD experiment. Temperature-programmed desorption mass spectra are recorded for HCN samples that are exposed to H atoms and those that are not. These spectra are normalized to take into account that slightly different quantities of HCN are deposited

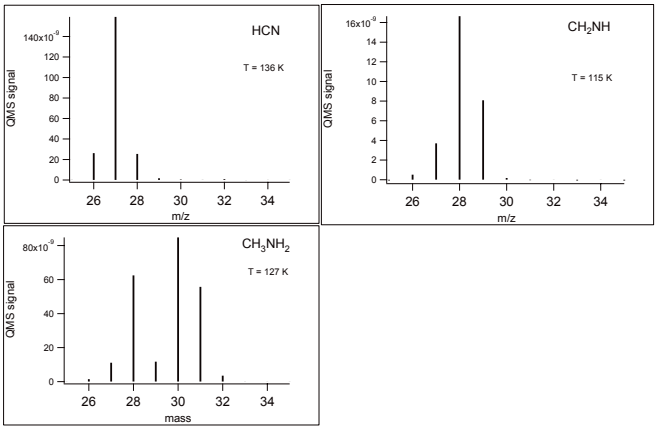

Fig. 2. Bar mass spectra of hydrogen cyanide HCN, methanimine CH_2NH, and methylamine CH_3NH_2 at T = 114 K, T = 115 K and T = 126 K respectively.

Table 1. Fundamental infrared band positions (cm^{-1}), with their assignments of HCN, CH_2NH and CH_2NH_3 at 10 K.

Vibration mode	HCN[a]	CH_2NH[b]	CH_3NH_2[c]
N-H_{as} stretch			3343
N-H_s stretch			3282
N-H stretch		3266	
C-H stretch	3118		
C-H_{as} stretch		3162/3140	2967/2942/2920
C-H_s stretch		2987/2916/2886	2897/2883/2862
C≡N stretch	2099		
C=N stretch		1642/1634	
NCH bend overtone	1628		
NH_2 bend			1615
CH_{3as} bend			1478/1455
CH_{3s} bend			1420
CH_2 scissoring		1411	
NH_2 torsion		1186	1339
CH_3 rocking			1156
NH torsion		1117	
C-N stretch			1042
NH_2 wagging			997/896
NCH bending	849		

References. [(a)] Gerakines et al. (2004); [(b)] Hamada et al. (1984); Jacox et al. (1975); [(c)] Bossa et al. (2008) .

from one experiment to another. For each experiment the HCN^+ molecular ion m/z 27 peak, which is not sensitive to any possible N_2 pollution, is integrated and the spectra of all masses are scaled by dividing them by the integration result. In this way can compare mass spectra originating from different experiments.

Figure 2 shows the relative intensities of the different masses in hydrogen cyanide HCN, methanimine CH_2NH, and methylamine CH_3NH_2 mass spectra for reference. HCN has a strong peak at m/z 27, CH_2NH has two strong peaks at m/z 28 and 29 and CH_3NH_2 has two strong peaks at m/z 30 and 31.

First Fig. 3 shows that there is a big change in the ice morphology. A TPD spectrum of bulk HCN, without H atoms bombardment, shows a clear zeroeth-order desorption curve. However, when exposed to the hydrogen beam, the zeroeth-order desorption curve is altered and shifted to higher temperature, and this change is function of the exposure time.

We can derive the amount of deposited HCN from IR spectra after deposition and prior H atoms bombardment by integrating the CN stretching band at 2099 cm^{-1}. A band strength of

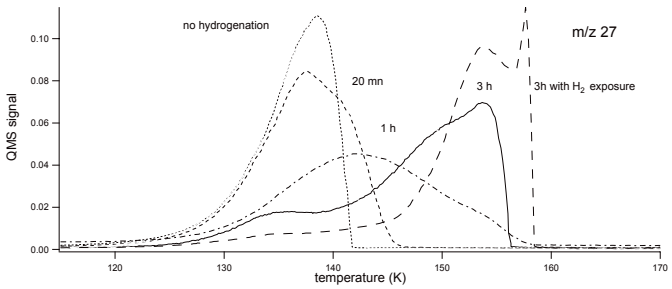

Fig. 3. Temperature-programmed desorption curves of m/z 27 of hydrogen cyanide HCN without exposure to the room-temperature atomic H-beam at 15 K (dotted line), and with exposure during 20 min (dashed line), one hour (dotted-dashed line) and three hours (full line). The warm atomic H_2 beam induces a change in morphology that shifts the desorption maximum to higher temperatures, as shown by the TPD curve obtained after three hours exposure to the H_2 beam with the plasma discharge off (large dashed line).

5.1×10^{18} cm molecule^{-1} is taken for this band (Gerakines et al. 2004). The ratio between the TPD spectrum m/z 27 integral and the IR spectrum at 2099 cm^{-1} band integral is the same for the unexposed sample and the different exposed samples. This means that the whole m/z band belongs to HCN and that the changes in the desorption curve do not correspond to the fragmentation of other heavier species. It also means that the hydrogenation yield is small, which explains that we cannot observe any hydrogenation products using IR spectroscopy. Therefore we conclude that the modified desorption curve of HCN is instead caused by a change in morphology than by a conversion in more saturated species.

This change in morphology of ice analogs after hydrogen atom exposure has already been shown (Accolla et al. 2010). Control experiments where the HCN ice is i. deposited at 15 K and kept at 15 K for three hours ii. deposited at 100 K iii. deposited at 15 K and then annealed at 100 K, give roughly similar TPD curves as the unexposed HCN ice. However, if the HCN ice is exposed to a pure H_2 beam (plasma discharge off) at 15 K for three hours, its TPD curve is similar to that of the HCN ice exposed to the hydrogen beam. This shows that the change in morphology in our experiment can be explained by the fact that warm H_2 molecules, which are the dominant species in the hydrogen beam, impinge on the 15 K surface, warm it up locally and change its morphology. This change in morphology could severely limit the yield of our hydrogenation experiments and may explain the low amount of hydrogenation products.

We then proceeded to identify the hydrogenation products. Figure 4 shows that peaks at m/z 30 and 31 are clearly visible in the HCN sample that was hydrogenated for 3 hours, while the unbombarded HCN sample does not have any isotopomer contribution at m/z 30 and 31. This shows that HCN is hydrogenated to methylamine CH_3NH_2, because CH_3NH_2 has its two most characteristic peaks at m/z 30 and 31, as seen in Fig. 2. This also implies that HCN must be first hydrogenated into intermediate species until the CH_3NH_2 fully saturated species.

Figure 5 shows the m/z 28 and 29 TPD curves without and with hydrogenation for different durations. The m/z 28 curve profile after hydrogen bombardment shows the change in morphology that the HCN sample undergoes. The unexposed HCN sample shows a peak at m/z 29 in the TPD curve, while the exposed HCN sample does not show any excess in the peak at m/z 29 after hydrogenation, which means that no CH_2NH has been formed. The m/z 29 peak of the unexposed sample can originate

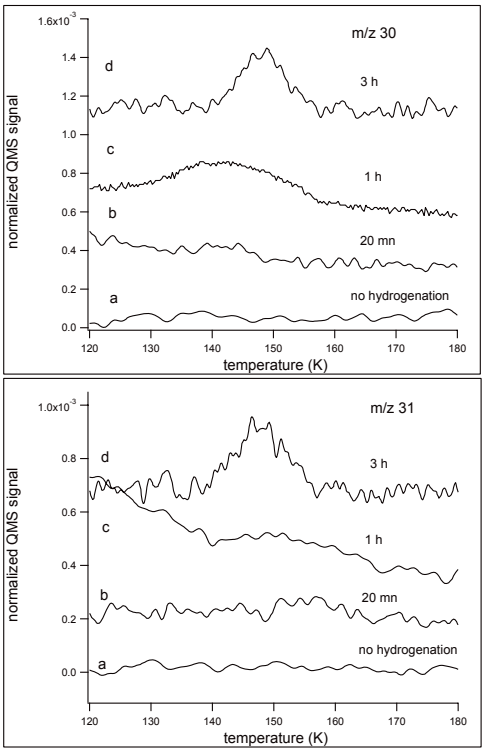

Fig. 4. Temperature-programmed desorption curve at m/z 30 and 31 of HCN without exposure to the atomic H beam (a) and after 20 min (b), 1 h (c) and 3 h (d) exposure at 15 K; m/z 30 and 31 evidence the formation of methylamine CH_3NH_2 from the hydrogenation of HCN.

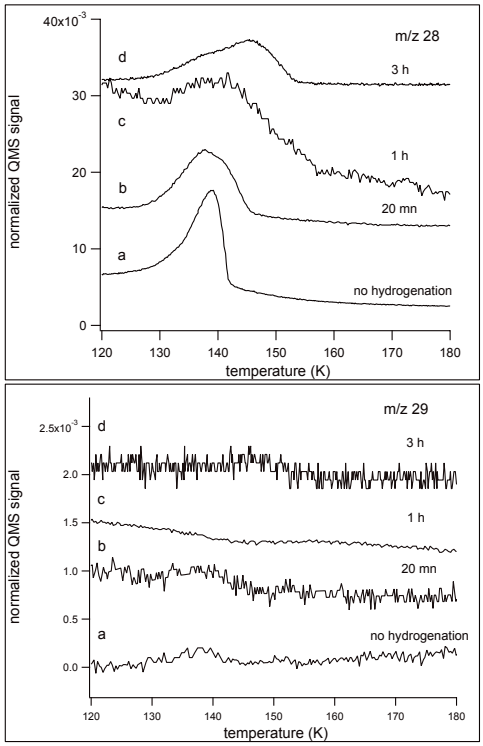

Fig. 5. Temperature-programmed desorption spectra of m/z 28 and 29 of HCN without exposure to the atomic H-beam at 15 K (a) and after 20 min (b), one hour (c), and three hours (d) exposure at 15 K; m/z 28 shows the change in morphology of HCN during the hydrogenation experiment. No contribution from CH_2NH is visible in the m/z 29 curve.

from the isotopomers bearing both ^{13}C and ^{15}N. However, the abundances of these isotopomers must be very low. Another possible origin for this peak is the ^{15}N-bearing N_2 isotopomer, which could originate from the N_2 deposited along with HCN or from the trapping at 15 K of the chamber residual N_2. However, the amount of $^{15}N_2$ must be extremely low as well. For the three hour long exposed HCN sample, we know from Fig. 2 that CH_3NH_2 m/z 29 peak must be approximately in a 1:10 ratio with its m/z 30 most intense peak, which is a very small contribution, in the noise of Fig. 5 m/z 29 TPD curve. Figure 2 shows that for CH_2NH the m/z 29 peak is in a 1:2 ratio with the m/z 28 peak, thus an excess on the m/z 29 peak should be clearly visible in Fig. 5 for the 3 h long exposed sample. We have not been able to observe this excess.

Thus we are not able to observe the CH_2NH intermediate HCN hydrogenation product, but we can observe the fully saturated CH_3NH_2 hydrogenation product only. Moreover no CH_2NH is present at intermediate exposure durations. After a 20 min hydrogenation neither CH_2NH nor CH_3NH_2 are formed. After a 1 h exposure, CH_3NH_2 is formed directly and no CH_2NH is detected. This could mean that the cross section for the second hydrogenation step, from methanimine CH_2NH to methylamine CH_3NH_2 is much larger than the first hydrogenation step, from HCN to CH_2NH, and that the second hydrogenation reaction is much faster. Both hydrogenation reactions could have an activation barrier and both hydrogenation could occur with trapped H atoms during the TPD experiment at temperature below the HCN thermal desorption. Thus, in both cases, it is difficult to observe the CH_2NH intermediate species.

3.2. Hydrogenation of methanimine CH_2NH

We want to check independently the CH_2NH to CH_3NH_2 second hydrogenation step. To this purpose we hydrogenate pure methanimine CH_2NH.

Gas-phase CH_2NH is condensed at 60 K on the copper surface to eliminate as much as residual NH_3. Figure 1 shows the IR spectrum of CH_2NH after deposition. Little NH_3 is present in our sample. The frozen solid is then exposed during two hours to the atomic hydrogen beam at 15 K. Then the sample is warmed to room temperature during a TPD experiment, with a 5 K/min temperature ramp rate. Figure 6 shows a TPD spectrum of CH_2NH with and without exposure to H atoms.

The hydrogenation experiment was performed twice to check for the reproductibility. The signal was normalized to the total amount of deposited CH_2NH. The two TPD experiments after hydrogenation were compared with a TPD experiment of a CH_2NH witness sample without hydrogenation. The m/z 30 peak shows the hydrogenation of CH_2NH into CH_3NH_2, but the witness sample also exhibits a smaller peak at m/z 30 caused by the $^{13}CH_2NH$ and $CH_2^{15}NH$ isotopomers. The formation of CH_3NH_2 is better shown by the peak at m/z 31, where the amount of isotopomers that both have a ^{13}C and a^{15}N is negligible. A TPD experiment of the sample holder exposed to the H-beam during two hours does not show any peak at m/z 30 or m/z 31. Therefore, we can conclude that CH_2NH can be hydrogenated into CH_3NH_2.

We note once again that the exposure to the atomic hydrogen beam has an effect on the physical structure of the CH_2NH solid. If it is not bombarded, CH_2NH desorbs with a typical zeroeth-order desorption shape. If bombarded by both H atoms and dominant warm H_2 molecules, the shape of the CH_2NH desorption

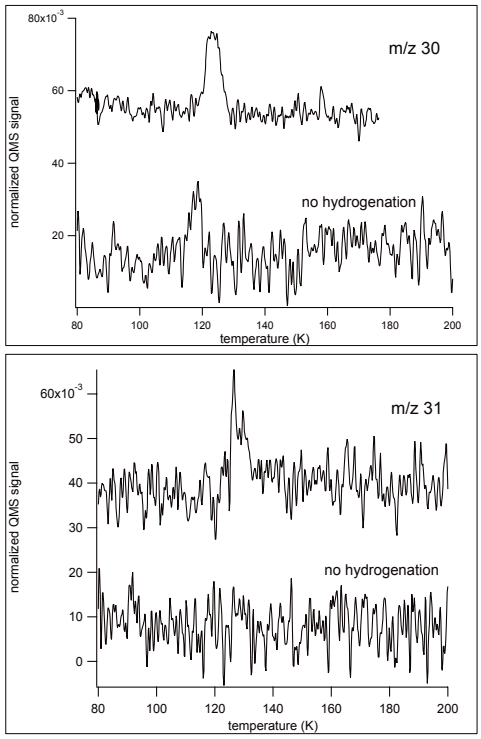

Fig. 6. Temperature-programmed desorption spectra of methanimine CH_2NH after hydrogenation for m/z 30 (*top*) and m/z 31 (*bottom*) at T = 15 K. The TPD spectrum of CH_2NH without hydrogenation is shown in the lower part of the figures for the two masses.

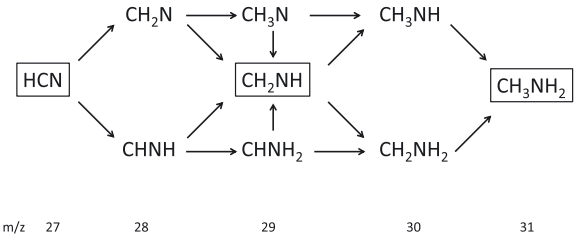

Fig. 7. Hydrogenation network of HCN at low temperature. Each arrow represents an hydrogen addition. The stable molecules are into frame. The other molecules are non-stable reaction intermediates.

curve is altered, and the desorption maximum is shifted to higher temperatures by approximately 5 K.

4. Discussion

We have carried out qualitative experiments of hydrogenation of hydrogen cyanide HCN and methanimine CH_2NH using a hydrogen plasma to generate atomic H, and TPD experiments to detect the hydrogenation products. From these experiments it is possible to draw a chemical reaction network for HCN hydrogenation at low temperature, below its thermal desorption, as shown in Fig. 7. Additional and more quantitative experimental work is needed to evaluate the cross-section of the different hydrogenation processes. However, we show the possibility to hydrogenate a C≡N bond until full saturation in interstellar conditions.

Although hydrogen cyanide HCN (Snyder et al. 1971), methanimine CH_2NH (Godfrey et al. 1973) and methylamine CH_3NH_2 (Kaifu et al. 1974; Fourikis et al. 1974) have been detected in the gas phase of the interstellar medium, there is no evidence so far of their presence in its solid-phase, which puts an upper limit detection to a few tenths of percents of solid H_2O. Solid-state HCN has been tentatively identified on Triton ices using the AKARI space telescope (Burgdorf et al. 2010) in its 2099 cm^{-1} band.

The feasibility of the HCN + H and CH_2NH + H to form CH_3NH_2 challenges the grain reaction scenario described in Garrod et al. (2008). The formation of CH_3NH_2 may be more likely to occur from accreted HCN hydrogenation than from the CH_3 + NH_2 reaction, because the H-atom residence time on the ice surface is significant at 10 K.

Moreover, CH_3NH_2 is important for the synthesis of amino-acids. It has been shown by Bossa et al. (2009) that the thermal reaction between CH_3NH_2 and CO_2 leads to the formation of methylammonium methylcarbamate $CH_3NH_3^+$,CH_3NHCOO^-, and that the VUV irradiation of this species can give the methylammonium glycinate $CH_3NH_3^+$,$NH_2CH_2COO^-$, which desorbs giving gas-phase glycine NH_2CH_2COOH. In that work CH_3NH_2 was supposed to be accreted onto the ice surface. Our work shows that CH_3NH_2 can be formed by direct hydrogenation of accreted HCN, which is a fairly abundant gas-phase species with a typical abundance of a few 10^{-9} with respect to H_2.

Methanimine CH_2NH is also a possible precursor for glycine. CH_2NH may react with HCN in an NH_3 environment (Danger et al. 2011) to form aminoacetonitrile NH_2CH_2CN, which is considered as a potential glycine precursor through the Strecker reaction in extraterrestrial objects such as meteorites and comets (Bernstein et al. 2002).

The non-observation of the hydrogenation intermediate species in HCN hydrogenation experiments must be discussed in more detail. Following the simple hydrogenation scheme presented in Fig. 7, there are three routes and three hydrogenation intermediate species possible to obtain CH_3NH_2 from HCN: a nitrene CH_3NH, a carbene $CHNH_2$, and a kinetically more stable species CH_2NH. Both CH_3NH and $CHNH_2$ must easily convert into the stable species CH_2NH. The non-observation of CH_2NH can be explained by a larger hydrogenation cross-section for CH_2NH than for HCN, so the intermediate CH_2NH is hydrogenated as soon as it is formed. The non-observation of CH_2NH can be also explained by the fact that the dominant branching ratio of the HCN hydrogenation is towards the nitrene CH_3NH and the carbene $CHNH_2$, and not to CH_2NH. Because these two species are more reactive, they hydrogenate easily into CH_3NH_2. Possibly the CH_3NH and $CHNH_2$ species can also react with the dominant species, remaining HCN, to form higher-mass species, like aminoacetonitrile NH_2CH_2CN (m/z 56, 55) or N-methylcyanamide CH_3NHCN. The reaction between intermediate species has been ruled out because we do not observe $m/z \geq 32$ in our TPD curves. This means that the non-observation of CH_2NH may be caused by the difference in hydrogenation cross-sections for the two hydrogenation steps.

5. Conclusion

We showed that hydrogen cyanide HCN can be hydrogenated to the fully saturated species methylamine CH_3NH_2 at low temperature. We propose a possible hydrogenation reaction scheme where methanimine CH_2NH is a stable intermediate. However, we cannot observe the hydrogenation of HCN into CH_2NH, whereas we observe the hydrogenation of CH_2NH into methylamine CH_3NH_2. This work shows that it is possible to hydrogenate a C≡N bond in interstellar conditions. Although more quantitative and detailed work needs to be carried out on the HCN hydrogenation scheme, on the relative cross-sections and

efficiencies, the saturation of HCN into CH_3NH_2 opens interesting perspectives on the formation of amino-acid precursors.

Acknowledgements. This work has been founded by the French national programme Physique Chimie du Milieu Interstellaire (PCMI) and the Centre National d'Études Spatiales (CNES). The authors would like to thank Prof. H. Cottin for the HCN synthesis protocol and the referee for the useful comments.

References

Accolla, M., Congiu, E., Dulieu, F., et al. 2010, Phys. Chem. Chem. Phys., 13, 8037
Bernstein, M. P., Dworkin, J. P., Sandford, S. A., Cooper, G. W., & Allamandola, L. J. 2002, Nature, 416, 401
Bisschop, S. E., Fuchs, G. W., van Dishoeck, E. F., & Linnartz, H. 2007, A&A, 474, 1061
Bossa, J. B., Borget, F., Duvernay, F., Theule, P., & Chiavassa, T. 2008, J. Phys. Chem. A, 112, 5113
Bossa, J. B., Duvernay, F., Theule, P., et al. 2009, A&A, 506, 601
Burgdorf, M., Cruikshank, D. P., Dalle Ore, C. M., et al. 2010, ApJ, 718, L53
Danger, G., Bossa, J.-B., de Marcellus, P., et al. 2011, A&A, 525, A30
Dulieu, F., Amiaud, L., Congiu, E., et al. 2010, A&A, 571, A30
Ferris, J. P., & Hagan, W. J. 1984, Tetrahedron, 40, 1093
Fehsenfeld, F. C., Evenson, K. M., & Broida, H. P. 1965, Rev. Sci. Instrum., 36, 294
Fourikis, N., Tagaki, K., & Morimoto, M. 1974, ApJ, 191, 139
Fuchs, G. W., Cuppen, H. M., Ioppolo, S., et al. 2009, A&A, 505, 629
Garrod, R. T., Weaver, S. L. W., & Herbst, E. 2008, ApJ, 682, 283
Gerakines, P. A., Moore, M. H., & Hudson, R. L. 2004, Icarus, 170, 202
Godfrey, P. D., Brown, R. D., Robinson, B. J., & Sinclair, M. W. 1973, Astrophys. Lett., 13, 119
Guillemin, J. C., & Denis , J. M. 1988, Tetrahedron, 44, 4431
Hamada, Y., Hashiguchi, K., Tsuboi, M., Koga, Y., & Kondo, S. 1984, J. Mol. Spec., 105, 70
Hiraoka, K., Ohashi, N., Kihara, Y., et al. 1994, Chemp. Phys. Lett., 229, 408
Hiraoka, K., Miyagoshi, T., Takayama, T., Yamamoto, K., & Kihara, Y. 1998, ApJ, 498, 710
Ioppolo, S., Cuppen, H. M., Romanzin, C., van Dishoeck, E. F., & Linnartz, H. 2008, ApJ, 686, 1474
Ioppolo, S., Cuppen, H. M., van Dishoeck, E. F., & Linnartz, H. 2010, MNRAS, 410, 1089
Jacox, M. E., & Milligan, D. E. 1975, J. Mol. Spec., 56, 333
Kaifu, N., Morimoto, M., Nagane, K., et al. 1974, ApJ, 191, 135
Matar, E., Congiu, E., Dulieu, F., Momeni, A., & Lemaire, J. L. 2008, A&A, 492, L17
Miyauchi, N., Hidaka, H., Chigai, T., et al. 2008, Chem. Phys. Lett., 456, 27
Mokrane, H., Chaabouni, H., Accolla, M., et al. 2009, ApJ, 705, L195
Romanzin, C., Ioppolo, S., Cuppen, H. M., van Dishoeck, E. F., & Linnartz, H. 2011, J. Chem. Phys., 134, 084504
Snyder, L. E., & Buhl, D. 1971, ApJ, 163, L47
Theule, P., Duvernay, F., Ilmane, A., et al. 2011, A&A, 530, A96
Watanabe, N., & Kouchi, A. 2002, ApJ, 571, L173